A New Buried-Oxide-In-Drift-Region Trench MOSFET With Improved Breakdown Voltage

Raghvendra Sahai Saxena, and M. Jagadesh Kumar, *Senior Member, IEEE*

***Abstract*—In this letter, we propose a new trench-gate power MOSFET with buried oxide in its drift region that shows an improvement in the breakdown performance as compared to the conventional trench device due to a reduction in the vertical electric field. In addition, the proposed device shows about linear relation between the BV and R_{ON} as compared to the 2.5th power relation in the conventional device.**

***Index Terms*—Breakdown voltage (BV), buried oxide (BOX), on-resistance, power MOSFET, trench gate.**

I. Introduction

In POWER MOSFETs, realizing low specific on-resistance (R_{ON}) and also high breakdown voltage (BV) is difficult because these two parameters are interlinked and improvement in one adversely affects the other. Usually, the on-resistance has 2.5th power dependence on the BV [1]. The superjunctions [2] and RESURF [3] structures are the most promising techniques to overcome this problem. In these techniques, the enhanced transverse electric field reduces the overall electric field, resulting in a near linear relation between R_{ON} and the BV.

In this letter, we propose the use of buried oxide (BOX) in the drift region of a trench-gate power MOSFET [4]–[8] near the trench sidewall that induces SOI–RESURF effect [3] and alters the current-conduction path at breakdown condition. Using 2-D numerical simulation [9], we show that the proposed device exhibits significantly larger BV for a given R_{ON} and an improved relation between BV and R_{ON} as compared to the conventional-device structure.

II. Device Structure and Fabrication Process

Fig. 1 shows the schematic cross-sectional view of the proposed device structure, termed in this letter as Buried-Oxide-In-Drift-region (BOXID) trench power MOSFET. A small part of the drift region, sandwiched between the trench and the BOX, carries the current and is denoted here as "active drift region."

The proposed fabrication-process steps of the BOXID device are shown in Fig. 2. We start with an N^+ substrate on which a 2.3-μm-thick N-type $(N_D = 10^{16}\ \mathrm{cm}^{-3})$ drift region and about

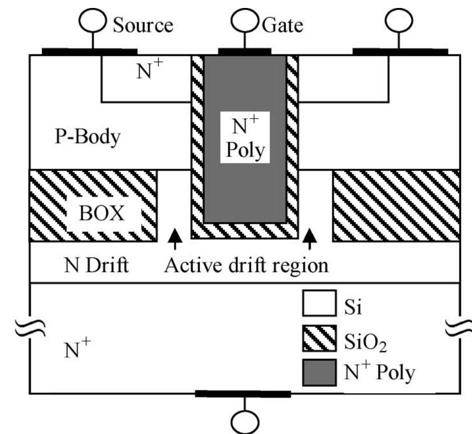

Fig. 1. Schematic cross-sectional view of the proposed BOXID device.

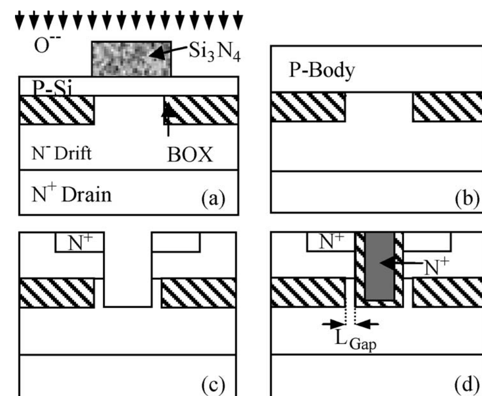

Fig. 2. Possible fabrication process of the BOXID device.

0.2-μm-thick P-type $(N_A = 5 \times 10^{17}\ \mathrm{cm}^{-3})$ region, respectively, are epitaxially grown. Using separation-by-implanted-oxygen process in specific areas, we selectively create the BOXID, as shown in Fig. 2(a). In this process, we implant the oxygen ions through a thin pad oxide layer except in the 1.2 μm × 1.2 μm-sized windows (protected by the Si_3N_4 mask) where we open the trenches later.

The implantation and annealing parameters are adjusted to create a 0.6-μm-thick BOX. Annealing also allows the crystallization of top P-surface. We further grow P–Si epitaxy to form a total of 0.6-μm-thick body region, as shown in Fig. 2(b). The N^+ source region $(N_D = 10^{19}\ \mathrm{cm}^{-3})$ of 0.1 μm is then created by implantation. We open 1.0-μm-wide and 1.2-μm-deep trenches in the middle of the BOX area, leaving about 0.1-μm lateral space from the BOX to the trench sidewalls from all the sides denoted by L_{Gap}, as shown in Fig. 2(c). In these

Manuscript received May 23, 2009; revised June 23, 2009. First published July 31, 2009; current version published August 27, 2009. This work was supported in part by the IBM Faculty Award. The review of this letter was arranged by Editor S.-H. Ryu.

The authors are with the Department of Electrical Engineering, Indian Institute of Technology, New Delhi 110 016, India (e-mail: rs_saxena@yahoo.com; mamidala@ieee.org).

Color versions of one or more of the figures in this letter are available online at http://ieeexplore.ieee.org.

Digital Object Identifier 10.1109/LED.2009.2026918

0741-3106/$26.00 © 2009 IEEE

Authorized licensed use limited to: INDIAN INSTITUTE OF TECHNOLOGY DELHI. Downloaded on August 26, 2009 at 22:53 from IEEE Xplore. Restrictions apply.

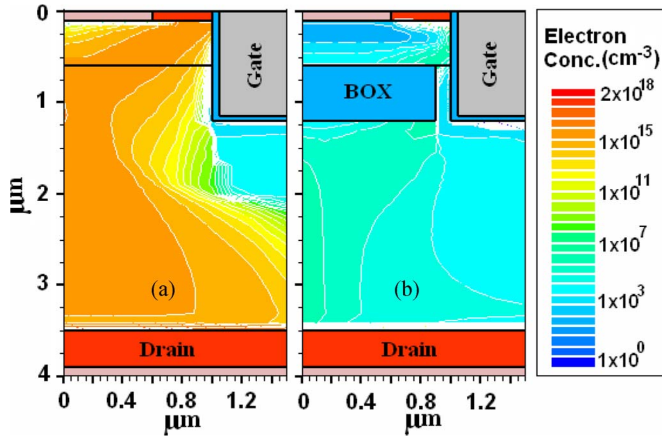

Fig. 3. Simulated electron concentration at $V_{\mathrm{DS}} = 192$ V in the structures of (a) conventional device and (b) BOXID device.

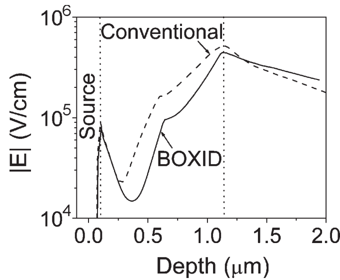

Fig. 4. Magnitude of electric field of the conventional and BOXID devices along the direction of current flow near the trench sidewall at $V_{\mathrm{DS}} = 192$ V.

trenches, we grow a 50-nm-thick gate oxide layer followed by deposition of N^+ poly and chemical mechanical polishing, as shown in Fig. 2(d). After making the metal contacts, the structure becomes like the one shown in Fig. 1.

III. Simulation Results and Discussion

We have created the BOXID device structure as well as the equivalent conventional-device structure (without BOX) in ATLAS [9]. Fig. 3(a) and (b) shows the left half of the device structures along with the electron-concentration contours. In the BOXID device, the passage of charge carriers at higher drain voltage is blocked by the BOX, and the complete active drift region gets depleted. As a result, similar to the SOI–RESURF effect [3], the vertical electric field, along the direction of the current flow, reduces, as shown in Fig. 4, resulting in enhanced BV.

A comparison of the breakdown performance of the BOXID and the conventional devices is shown in Fig. 5(a) showing an increase in BV from 192 to 430 V (~124% improvement).

The blocking of the current-conduction path may result in the reduction of current and, therefore, a higher R_{ON}. The heat dissipation and oxide defects are the other problems with the BOXID. However, since the current mostly passes near the trench sidewalls in ON-state, even after blocking about 90% of the drift region, only an 11% decrease is observed in the drive current of the BOXID device as compared to the conventional device, as depicted by the $I_{\mathrm{DS}}-V_{\mathrm{GS}}$ characteristics shown in Fig. 5(b). In addition, due to the current being confined near the trench sidewalls, the heat is generated near the sidewalls and may be dissipated via heat flow paths to source and drain [8], and thus, heat dissipation is also not a severe problem. The fixed oxide charges may degrade the BV of the device due to charge imbalance but that may be compensated, as illustrated in [10].

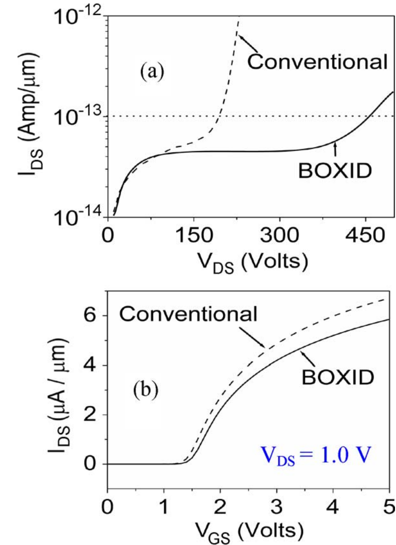

Fig. 5. Comparison of (a) breakdown performance and (b) typical $I_{\mathrm{DS}}-V_{\mathrm{GS}}$ characteristics of the BOXID and conventional devices for $V_{\mathrm{DS}} = 1.0$ V.

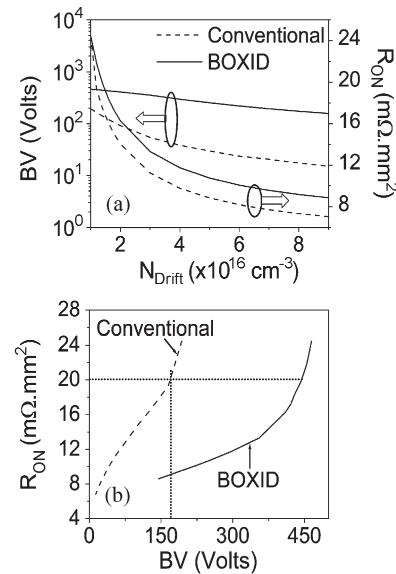

Fig. 6. Comparison of (a) BV and R_{ON} with varying drift-region doping and (b) R_{ON} versus BV for the BOXID and conventional devices.

To examine the relation between R_{ON} and the BV, we have changed the drift-region doping from 1×10^{16} to 1×10^{17} cm^{-3} and compared the R_{ON} and breakdown performance of the BOXID device and the conventional device. Fig. 6(a) shows the dependence of BV and R_{ON} on the drift-region doping. It may be noticed that the degradation in BV with respect to the drift-region doping is less in the BOXID device as compared to the conventional device, whereas change in R_{ON} is almost similar in both devices. This results in a better relation between R_{ON} and the BV in the BOXID device as compared to the conventional device. Fig. 6(b) shows that the slope of R_{ON}

Authorized licensed use limited to: INDIAN INSTITUTE OF TECHNOLOGY DELHI. Downloaded on August 26, 2009 at 22:53 from IEEE Xplore. Restrictions apply.

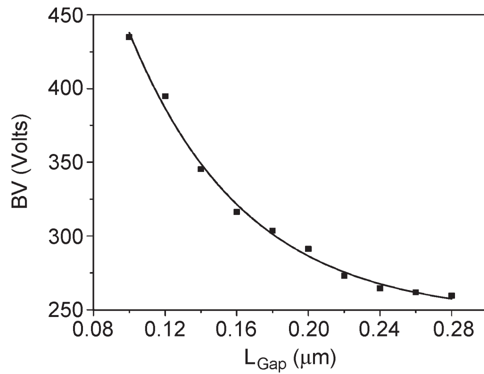

Fig. 7. BV dependence on L_{Gap}.

versus BV curve is significantly smaller in the BOXID device as compared to the conventional device, and nonlinear curve fitting shows that the R_{ON} has, on an average, 1.6th power relation with BV in the BOXID device in contrast with the 2.5th power relation in the conventional device.

From Fig. 6(b), it may be inferred that, for a target R_{ON} of 20 $\mathrm{m}\Omega \cdot \mathrm{mm}^2$, the BV of the BOXID device will be 440 V as compared to 170 V of the conventional device. Similarly, for a target BV $=$ 170 V, the R_{ON} value of the BOXID and the conventional devices will be 9 and 20 $\mathrm{m}\Omega \cdot \mathrm{mm}^2$, respectively. Thus, we see that the presence of the BOX in the drift region results in a significant improvement in the performance of trench power MOSFETs.

The improvement in BV is a function of the separation length L_{Gap} between the trench sidewall and the BOX. The BV decreases when L_{Gap} increases, as shown in Fig. 7. This indicates that any misalignment of trench with respect to the BOX, causing an increase in L_{Gap} at one side of the trench, results in a reduced BV. A 50% misalignment may reduce the BV by about 30%. However, the improvement in BV is still significant as compared to the conventional device.

IV. Conclusion

In this letter, a new BOXID trench MOSFET has been proposed in which a BOX layer in the drift region blocks the major current-conduction path during breakdown and also helps to sustain more drain voltage due to the enhanced RESURF effect. This letter indicates that nearly 124% improvement can be realized in the OFF-state BV in the proposed device as compared with the conventional trench MOSFET. We have also shown that the relation between R_{ON} and BV is improved from 2.5th to 1.6th power relation.

References

[1] R. P. Zingg, "On the specific on-resistance of high-voltage and power devices," *IEEE Trans. Electron Devices*, vol. 51, no. 3, pp. 492–499, Mar. 2004.

[2] Y. Chen, Y. C. Liang, G. S. Samudra, X. Yang, K. D. Buddharaju, and H. Feng, "Progressive development of superjunction power MOSFET devices," *IEEE Trans. Electron Devices*, vol. 55, no. 1, pp. 211–219, Jan. 2008.

[3] M. Kanechika, M. Kodama, T. Uesugi, and H. Tadano, "A concept of SOI RESURF lateral devices with striped trench electrodes," *IEEE Trans. Electron Devices*, vol. 52, no. 6, pp. 1205–1210, Jun. 2005.

[4] M. Li, A. Crellin, I. Ho, and Q. Wang, "Double-epilayer structure for low drain voltage rating n-channel power trench MOSFET devices," *IEEE Trans. Electron Devices*, vol. 55, no. 7, pp. 1749–1755, Jul. 2008.

[5] R. S. Saxena and M. J. Kumar, "A stepped oxide hetero-material gate trench power MOSFET for improved performance," *IEEE Trans. Electron Devices*, vol. 56, no. 6, pp. 1355–1359, Jun. 2009.

[6] R. S. Saxena and M. J. Kumar, "Dual material gate technique for enhanced transconductance and breakdown voltage of trench power MOSFETs," *IEEE Trans. Electron Devices*, vol. 56, no. 3, pp. 517–522, Mar. 2009.

[7] R. S. Saxena and M. J. Kumar, "A new strained-silicon channel trench-gate power MOSFET: Design and analysis," *IEEE Trans. Electron Devices*, vol. 55, no. 11, pp. 3229–3304, Nov. 2008.

[8] J. Roig, I. Cortés, D. Jiménez, D. Flores, B. Iñiguez, S. Hidalgo, and J. Rebollo, "A numerical study of scaling issues for trench power MOSFETs," *Solid State Electron.*, vol. 49, no. 6, pp. 965–975, Jun. 2005.

[9] *Atlas User's Manual: Device Simulation Software*. Santa Clara, CA: Silvaco Int., 2008.

[10] S. Balaji and S. Karmalkar, "Effects of oxide-fixed charge on the breakdown voltage of superjunction devices," *IEEE Electron Device Lett.*, vol. 28, no. 3, pp. 229–231, Mar. 2007.

Authorized licensed use limited to: INDIAN INSTITUTE OF TECHNOLOGY DELHI. Downloaded on August 26, 2009 at 22:53 from IEEE Xplore. Restrictions apply.